Oceanic effects on polar motion determined from an ocean model and satellite altimetry: 1993–2001

J.-L. Chen and C. R. Wilson[1]
Center for Space Research, University of Texas at Austin, Austin, Texas, USA

X.-G. Hu and Y.-H. Zhou
Shanghai Astronomical Observatory, Chinese Academy of Sciences, Shanghai, China

B. D. Tapley
Center for Space Research, University of Texas at Austin, Austin, Texas, USA

Received 30 June 2003; revised 17 November 2003; accepted 15 December 2003; published 26 February 2004.

[1] Mass redistribution and motion in the oceans are major driving forces of geodetic variations, including polar motion, length of day, geocenter, and gravity field changes. We examine oceanic contribution to polar motion using estimates from a data-assimilating ocean general circulation model and satellite radar altimeter observations. The data include model estimates of variations in oceanic mass (OBP) and meridional and zonal velocities. Sea level anomalies from TOPEX/Poseidon (T/P) satellite altimeter measurements and steric sea surface height changes deduced from the model are also used to estimate OBP effects. Estimated oceanic contributions from both the model and T/P show considerably better agreement with polar motion observations compared with results from previous studies. The improvement is particularly significant at intraseasonal timescales. Both OBP and ocean current variations provide important contributions to polar motion. At intraseasonal timescales the oceans appear to be a dominant contributor to residual polar motion not accounted for by the atmosphere. The oceans also play an important role in seasonal excitation. Combined OBP and ocean current contributions explain much of the residual semiannual variability. *INDEX TERMS:* 1223 Geodesy and Gravity: Ocean/Earth/atmosphere interactions (3339); 1239 Geodesy and Gravity: Rotational variations; 4283 Oceanography: General: Water masses; 4512 Oceanography: Physical: Currents; 4556 Oceanography: Physical: Sea level variations; *KEYWORDS:* polar motion, OGCM, satellite altimeter, ocean

Citation: Chen, J.-L., C. R. Wilson, X.-G. Hu, Y.-H. Zhou, and B. D. Tapley (2004), Oceanic effects on polar motion determined from an ocean model and satellite altimetry: 1993–2001, *J. Geophys. Res.*, *109*, B02411, doi:10.1029/2003JB002664.

1. Introduction

[2] At timescales of a few years and less, Earth's rotational changes (polar motion X and Y and length of day (LOD)) are primarily driven by air and water mass redistribution and movement within the Earth system. Atmospheric winds and surface pressure changes are considered to be the dominant contributors to LOD variation [e.g., *Barnes et al.*, 1983; *Eubanks et al.*, 1988; *Hide and Dickey*, 1991] and are responsible for a portion of observed polar motion [e.g., *Chao and Au*, 1991]. Water mass redistribution within the oceans and continental water storage change are also believed to play major roles, particularly for polar motion. Previous studies based on various ocean models [e.g., *Dickey et al.*, 1993; *Ponte et al.*, 1998, 2001; *Johnson et al.*, 1999; *Ponte and Ali*, 2002; *Gross et al.*, 2003] and satellite radar altimeter measurements [e.g., *Chen et al.*, 2000a] all demonstrate that the oceans provide important contributions to the excitation of polar motion. However, clear quantitative understanding of oceanic effects on polar motion and LOD remains a challenging goal. A fundamental limitation is the scarcity of observations of the global oceans, which translates into relatively large uncertainties in predictions of ocean general circulation models (OGCM). The two oceanic contributions are from variations in currents and ocean bottom pressure (OBP), and of these, OBP effects are probably the most difficult to estimate [e.g., *Ponte and Stammer*, 1999; X. G. Hu et al., Ocean bottom pressure variability: A study with ocean general circulation models, satellite altimetry, and in situ measurements, submitted to *Journal of Geodesy*, 2003]. Although satellite altimeters provide nearly global sea surface height (SSH) changes, estimating OBP from them requires removal of steric sea level variations, which are poorly known [e.g., *Chen et al.*, 2000a, 2000b].

[3] Recent advancements in data-assimilating OGCMs have inspired new studies of oceanic effects on Earth's

[1] Also at Department of Geological Sciences, University of Texas at Austin, Austin, Texas, USA.

0148-0227/04/2003JB002664$09.00

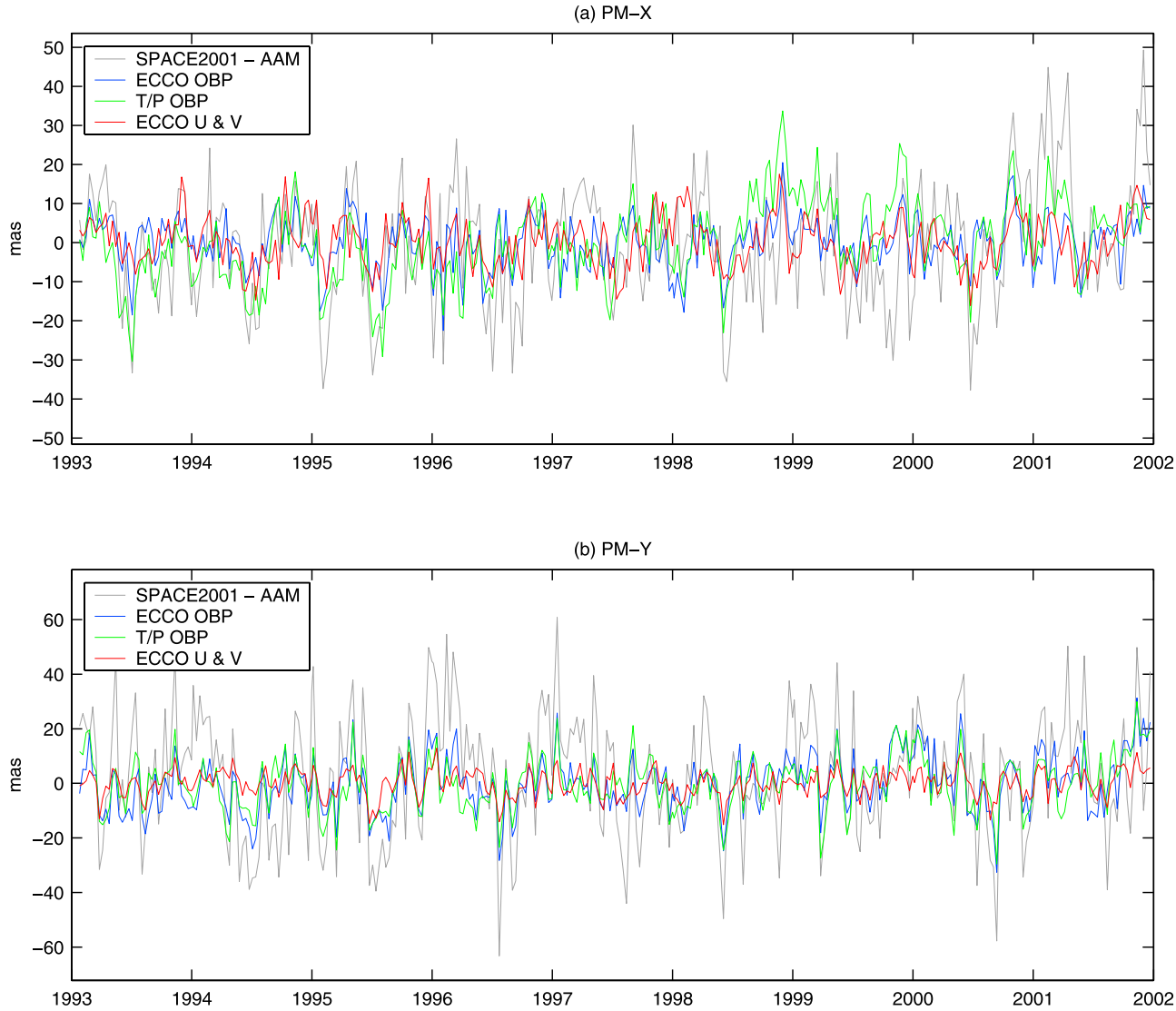

Figure 1. Oceanic excitations on polar motion (a) *X* and (b) *Y* from Estimating the Circulation and Climate of the Ocean (ECCO) ocean bottom pressure (OBP) (blue curves), TOPEX/Poseidon (T/P)-derived OBP (green curves), and ECCO ocean current (red curves), compared with SPACE2001 minus National Centers for Environmental Prediction (NCEP) atmospheric angular momentum (AAM) (gray curves).

rotation and gravity field [*Ponte et al.*, 2001; *Dickey et al.*, 2002; *Chen et al.*, 2003; *Gross et al.*, 2003]. The data-assimilating OGCM [*Fukumori et al.*, 2000] developed at NASA's Jet Propulsion Laboratory (JPL), a partner in the Estimating the Circulation and Climate of the Ocean (ECCO) program, provides near real-time estimates of physical changes, including current, SSH, temperature (T), salinity (S), and OBP. The ECCO model calculations are thus a valuable resource in the study of oceanic effects on geodetic observations, and ECCO estimates of T and S provide the information needed to calculate steric SSH changes caused by seawater density variations.

[4] The TOPEX/Poseidon (T/P) satellite radar altimeter and its follow-on Jason-1 have been producing accurate global measurements of SSH every 10 days for over 10 years. T/P SSH changes include two effects: steric changes that do not alter OBP and mass changes that do. Using T/P SSH data from 1993 to 1996 and a simplified steric SSH model from ocean temperature data taken over many years, *Chen et al.* [2000a] showed that the oceans may play an important role in driving intraseasonal polar motion. However, their conclusions were limited in part by the relatively short duration of T/P data and, more importantly, by the steric SSH model, which was purely seasonal. A new study of the altimeter data is called for, given the extended period of T/P observations, and the ECCO OGCM which is suitable for estimating time series of steric SSH.

[5] In this study, we investigate oceanic effects on polar motion using ECCO and T/P results at seasonal and shorter timescales. ECCO estimates of OBP and currents provide one estimate of the entire ocean contribution, while T/P SSH combined with ECCO SSH predictions provide a second OBP estimate. We have not extended the study to

Table 1. Amplitude and Phase of Annual and Semiannual Polar Motion Excitations (X, Y) From Observations (SPACE2001-AAM), ECCO, and T/P Predictions[a]

	X Annual		X Semiannual		Y Annual		Y Semiannual	
Polar Motion (X, Y)	Amplitude, mas	Phase, deg	Amplitude, mas	Phase, deg	Amplitude, mas	Phase, deg	Amplitude, mas	Phase, deg
SPACE2001-AAM	7.71	52.1	6.14	250.0	13.50	49.6	3.89	174.1
ECCO OBP	2.05	147.8	2.79	238.9	1.50	72.8	2.24	214.6
T/P OBP	5.26	117.0	4.01	252.2	4.57	130.1	0.93	205.0
ECCO U and V	5.01	99.0	2.52	246.6	5.72	79.8	2.25	219.4
ECCO OBP and U and V	6.62	112.5	5.29	242.6	7.21	78.4	4.49	217.0
T/P OBP and ECCO U and V	10.22	108.2	6.52	250.1	5.53	116.9	3.17	211.8
OAM [*Gross et al.*, 2003]	4.75	100.7	5.03	240.1	8.43	71.3	2.22	231.5

[a]The phase is defined as ϕ in $\sin(2\pi(t - t_0) + \phi)$, where t_0 refers to 0000 UT on 1 January. Similar estimates from the OAM time series of *Gross et al.* [2003] are also listed for comparison. Abbreviations are AAM, atmospheric angular momentum; ECCO, Estimating the Circulation and Climate of the Ocean; T/P, TOPEX/Poseidon; OBP, ocean bottom pressure; OAM, oceanic angular momentum; and mas, milliseconds of arc.

LOD because in that case the winds are the dominant excitation source.

2. Theory

[6] Polar motion is excited by mass motion (e.g., winds and currents) and surface mass load (e.g., atmospheric pressure and OBP) variations. The two components of polar motion excitations, χ_1 and χ_2, can be represented as the sum of these two terms,

$$\begin{bmatrix} \chi_1 \\ \chi_2 \end{bmatrix} = \begin{bmatrix} \chi_1^{\text{mass}} \\ \chi_2^{\text{mass}} \end{bmatrix} + \begin{bmatrix} \chi_1^{\text{motion}} \\ \chi_2^{\text{motion}} \end{bmatrix}. \tag{1}$$

[7] At a given grid point (latitude ϕ, longitude λ, and time t), OBP change represents the integral of mass change of the water column above and can be approximately treated as mass load change, $q(\phi, \lambda, t) = \Delta\text{OBP}/g$ (in units of kg/m^2, where g is gravitational acceleration). Therefore oceanic excitation of polar motion can be computed as [e.g., *Eubanks*, 1993]

$$\begin{bmatrix} \chi_1^{\text{mass}} \\ \chi_2^{\text{mass}} \end{bmatrix} = -\frac{1.098 R_E^2}{(C - A)} \int\int \text{q}(\phi, \lambda, \text{t}) \sin(\phi) \cos(\phi) \begin{bmatrix} \cos(\lambda) \\ \sin(\lambda) \end{bmatrix} \text{ds} \tag{2}$$

$$\begin{bmatrix} \chi_1^{\text{motion}} \\ \chi_2^{\text{motion}} \end{bmatrix} = \frac{1.5913 \text{R}_\text{E}}{(\text{C} - \text{A})\Omega_0} \int\int\int \cdot \cos(\phi) \left(\text{U}(\phi, \lambda, \text{h}, \text{t}) \begin{bmatrix} -\cos(\lambda)\sin(\phi) \\ -\sin(\lambda)\sin(\phi) \end{bmatrix} + \text{V}(\phi, \lambda, \text{h}, \text{t}) \begin{bmatrix} \sin(\lambda) \\ -\cos(\lambda) \end{bmatrix} \right) \text{dm}, \tag{3}$$

in which R_E and Ω_0 are the Earth's mean radius and angular velocity, respectively, A and C are the Earth's principal moments of inertia, and U and V are the zonal and meridional velocities of currents, respectively. The surface area element is $ds = R_E^2 \cos(\phi) d\phi d\lambda$, and $dm = \rho R_E^2 \cos(\phi) d\phi d\lambda dh$ is the mass element of a given grid box. The density of seawater is ρ, the layer depth is h, and the layer thickness is dh. Since density only changes slightly with temperature, salinity, and pressure change (typically below the 1% level), we use a constant mean density (ρ_0 = 1.028 g/cm^3) in computing ocean current excitations.

3. Data and Models

3.1. ECCO/JPL Model

[8] The ECCO OGCM is based on the parallel version of the Massachusetts Institute of Technology general circulation model and an approximate Kalman filter method [*Fukumori et al.*, 2000]. The ECCO model (run kf047a) assimilates T/P SSH observations. The model coverage is nearly global from −79.5°S to 78.5°N and has a telescoping meridional grid with a 1/3° resolution in the tropics (−20°S to 20°N) that gradually increases to a 1° resolution away from the equator. The resolution in longitude is 1°. There are 46 vertical levels with 10-m resolution within 150 m of the surface. The model is forced by National Centers for Environmental Prediction (NCEP) reanalysis products [*Kalnay et al.*, 1996] (12-hour interval wind stress data and daily heat and fresh water fluxes) with time means replaced by those of the Comprehensive Ocean-Atmosphere Data Set. Temperature and salinity at the model sea surface are relaxed toward observed values. Model fields are available at 10-day intervals (as 10-day averages). SSH and OBP are also available at 12-hour intervals (as instantaneous values).

[9] The ECCO values used here include 10-day averaged OBP, SSH, zonal (U), and meridional (V) velocities from January 1993 to December 2001. We use ECCO T and S changes to estimate steric SSH change and to provide a correction for T/P SSH. The ECCO model employs the Bossiness approximation to conserve total ocean volume. This will cause changes of estimated total ocean mass unrelated to any oceanographic effect. To correct this, we enforce ECCO mass conservation by removing a mean OBP (over the oceans) at each time step [*Greatbatch*, 1994]. This correction is not required for T/P-derived OBP change because T/P measures real sea level change, including effects of water exchange between the oceans and other elements of the Earth system [e.g., *Chen et al.*, 1998; *Minster et al.*, 1999].

3.2. T/P SSH Observations and ECCO Steric Estimates

[10] T/P SSH data are from the *Jet Propulsion Laboratory* [2002]. The data are given on a 1° by 1° grid (via Gossip interpolation) every 5 days from October 1992 to

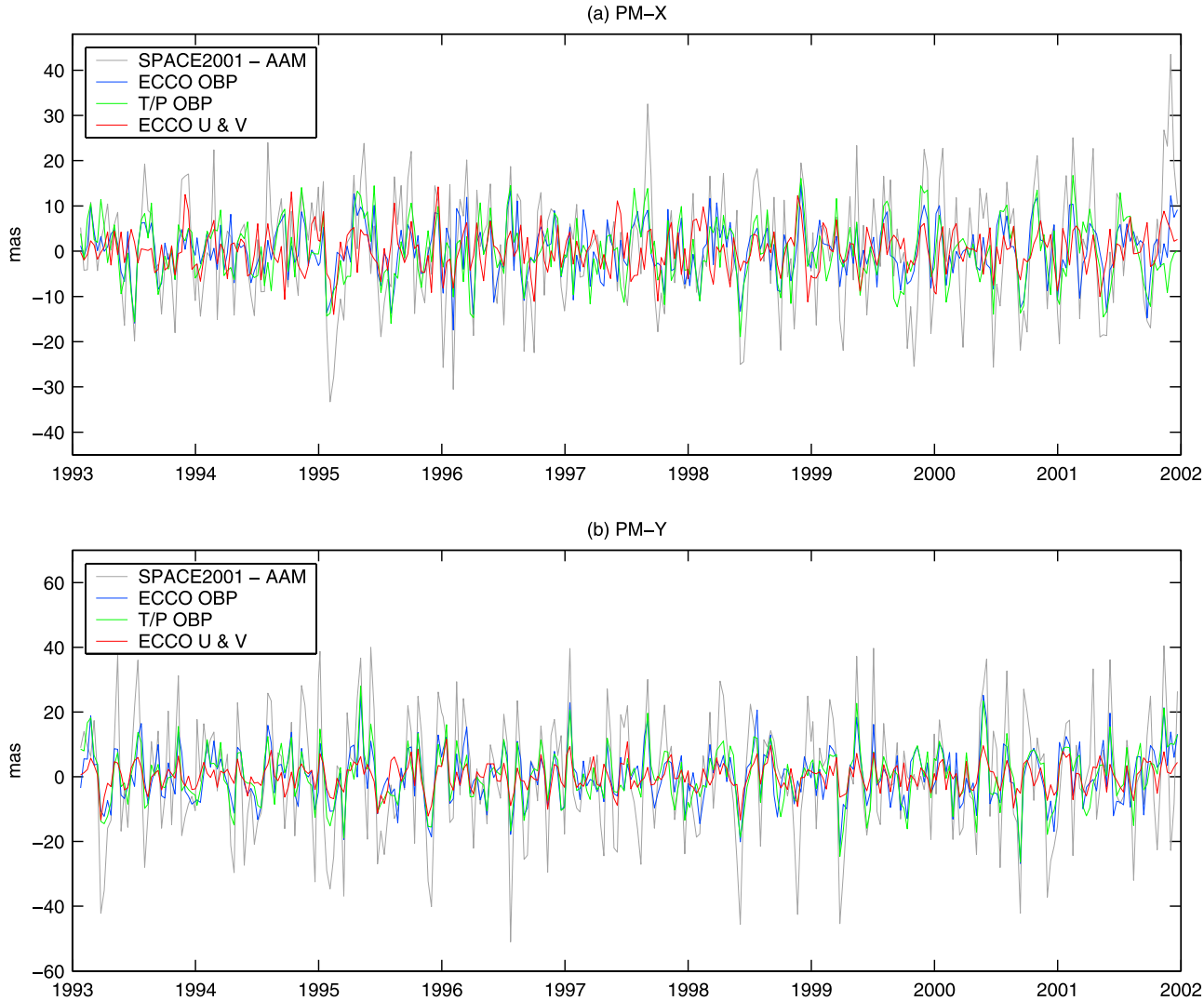

Figure 2. Intraseasonal oceanic excitations on polar motion (a) X and (b) Y from ECCO OBP (blue curves), T/P-derived OBP (green curves), and ECCO ocean current (red curves), compared with SPACE2001-NCEP AAM (gray curves).

December 2001. The portion overlapping the ECCO results (January 1993 to December 2001) is used here. We resampled the T/P data to the ECCO 10-day interval. Atmospheric inverted barometer (IB) effects on sea level change have been corrected using NCEP reanalysis surface pressure data (see details at http://podaac.jpl.nasa.gov/woce/woce3_topex/topex/docs/topex_doc.htm).

[11] OBP variations are the difference between SSH and steric SSH change [e.g., *Chen et al.*, 2000b], so $\Delta\mathrm{OBP} = g\rho_0(\mathrm{SSH} - \mathrm{SSH}_{\mathrm{steric}})$, where

$$\mathrm{SSH}_{\mathrm{steric}} = -\frac{1}{\rho_0}\int_{-h}^{0} \Delta\rho\, dh \qquad (4)$$

and where $\Delta\rho$ is the density change as a function of T, S, and pressure (P). The integral is from the ocean bottom to the surface ($h = 0$). $\Delta\rho$ is computed using the UNESCO 1983 algorithm [*Fofonoff and Millard*, 1983]. Using equation (4), we compute $\mathrm{SSH}_{\mathrm{steric}}$ using T, S, and P (P is inferred from layer depths) from the ECCO model and then combine them with T/P data.

3.3. Polar Motion Observations and Atmospheric Effects

[12] Polar motion X and Y time series are from SPACE2001 [*Gross*, 2002], obtained from various space geodetic observations (very long baseline interferometry, GPS, satellite laser ranging, and lunar laser ranging) through a Kalman filter combination [*Eubanks*, 1988]. The data cover the period September 1976 through January 2002, with daily sampling. X and Y time series are averaged and resampled at the same 10-day interval as ECCO results. Subdaily tidal corrections have been removed from X and Y series [*Gross*, 2002]. Polar motion excitations χ_1 and χ_2 are derived from X and Y using the discrete polar motion equation of *Wilson* [1985].

[13] Atmospheric wind and surface pressure effects on χ_1 and χ_2 are removed using NCEP reanalysis atmo-

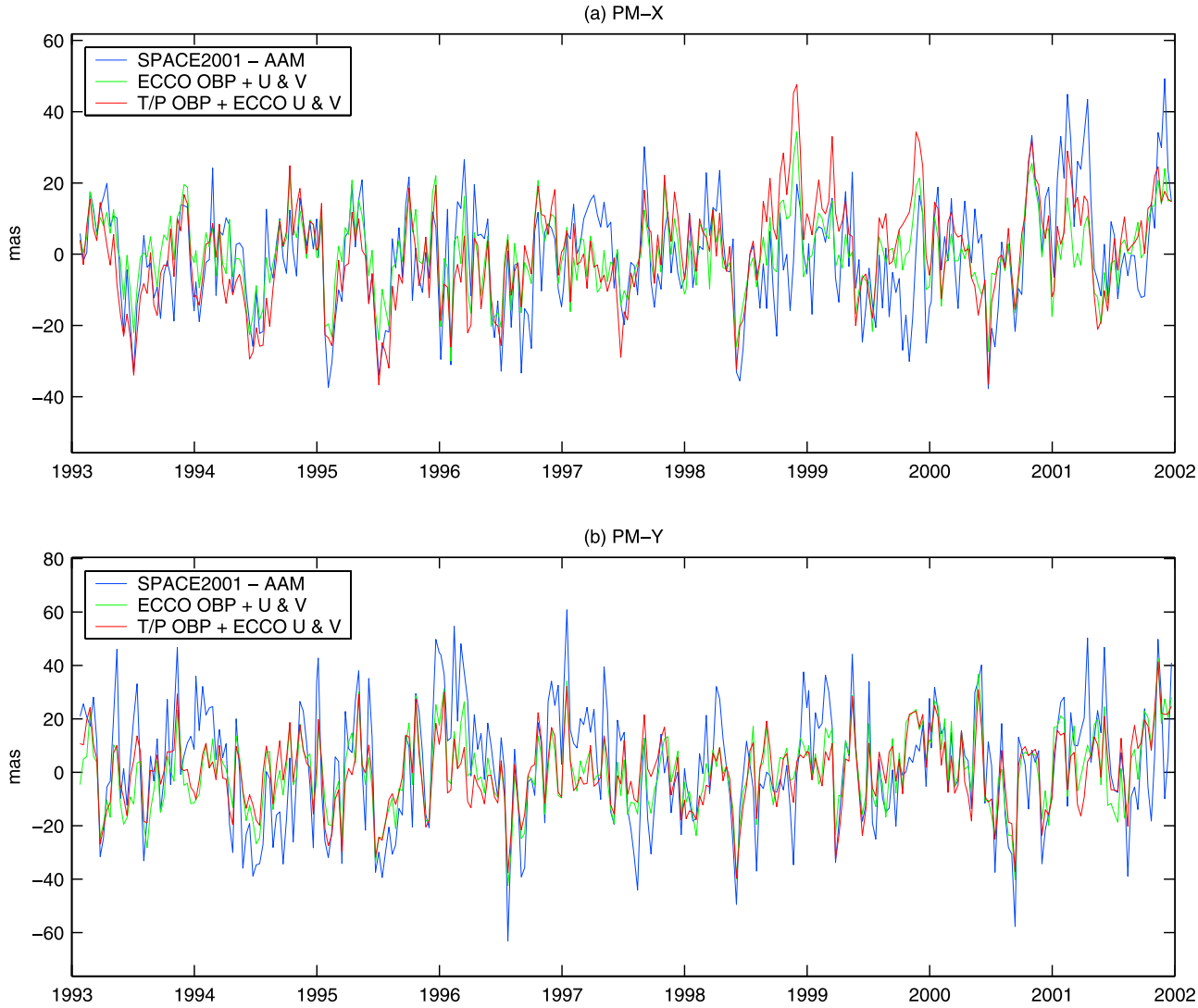

Figure 3. Combined oceanic effects on polar motion (a) X and (b) Y from ECCO OBP plus U and V (green curves) and T/P OBP plus ECCO U and V (red curves), compared with SPACE2001-NCEP AAM (blue curves).

spheric angular momentum (AAM) results provided by atmospheric and environmental research [*Salstein and Rosen*, 1997]. IB effects are corrected in the same way as for T/P SSH data. Wind excitations are computed by integrating the horizontal winds from the surface to the top of the model at 10 hPa. The daily excitations from SPACE2001 and 6-hour interval AAM time series are averaged and resampled at the same 10-day intervals as the ECCO model. Residuals after subtracting atmospheric effects are expected to be dominantly due to the oceans and continental water storage changes.

4. Results and Comparison

4.1. Contributions From OBP Change

[14] Oceanic contributions to X and Y from ECCO OBP are shown in Figures 1a and 1b (blue curves). The residual variations of X and Y (i.e., SPACE2001 minus atmospheric effects) are in gray. Figures 1a and 1b also show (green curves) contributions from T/P-derived OBP change. Clearly, oceanic mass redistribution (OBP changes) is responsible for a significant portion of residual X and Y variations over a broad band of frequencies. Both ECCO and T/P predictions agree reasonably well with the residuals.

[15] To have a closer look at seasonal frequencies, we estimate amplitudes and phases of annual and semiannual variations from time series in Figure 1 by least squares, with results shown in Table 1. OBP change is an important source of seasonal polar motion. T/P OBP predicts relatively larger annual and semiannual changes in X compared with ECCO but smaller changes in Y. The phases of the semiannual terms agree very well (see Table 1), although agreement of annual phases is relatively poor. We removed annual and semiannual sinusoidal terms and signals with periods of 1 year and longer from all time series and show the remaining intraseasonal variations in Figures 2a and 2b. Agreement between polar motion observations and OBP predictions is evident.

4.2. Contributions From Ocean Current

[16] Contributions from ECCO ocean currents (U and V) are shown in red in Figures 1a and 1b, with intraseasonal

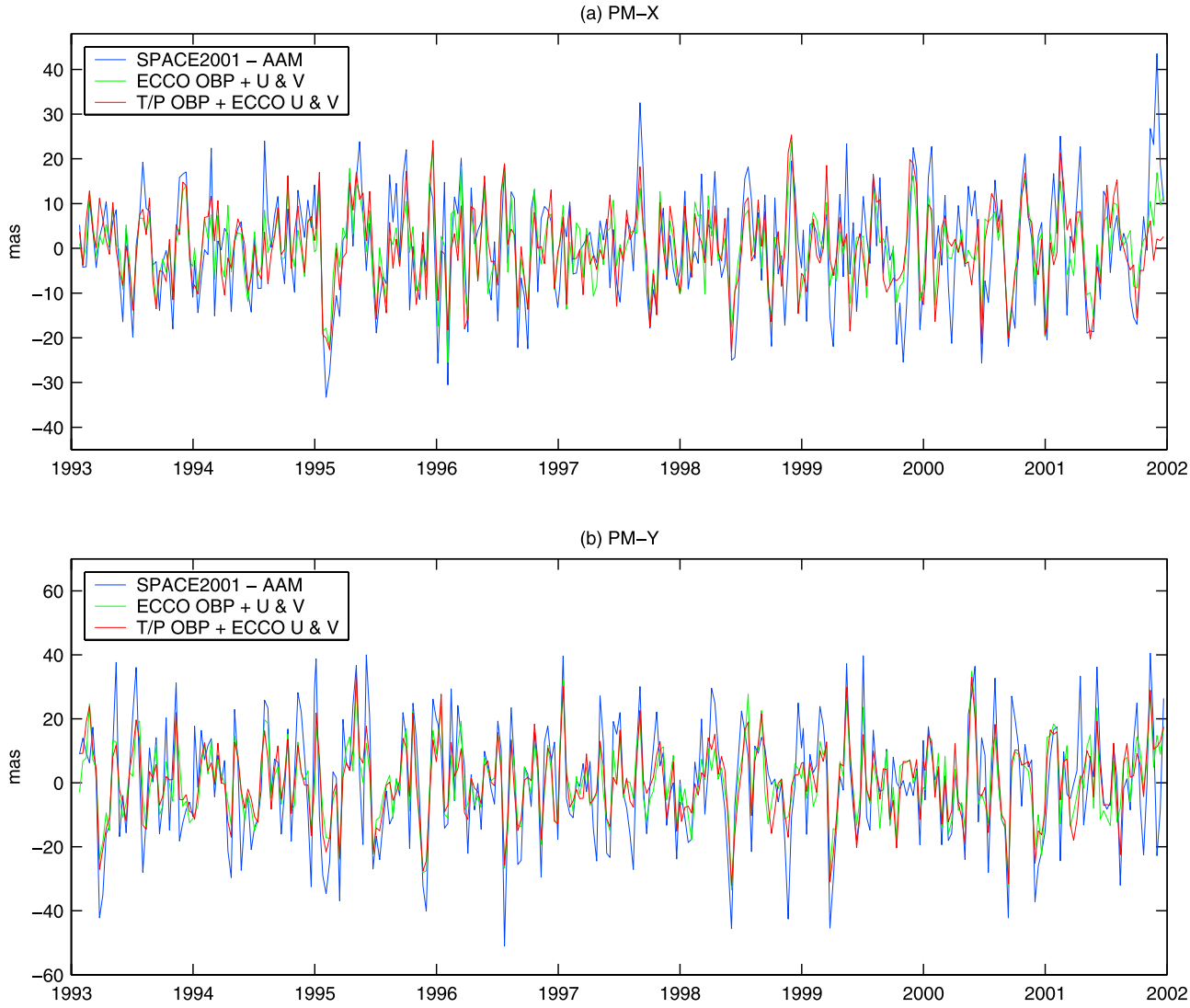

Figure 4. Intraseasonal combined oceanic effects on polar motion (a) X and (b) Y from ECCO OBP plus *U* and *V* (green curves) and T/P OBP plus ECCO *U* and *V* (red curves), compared with SPACE2001-NCEP AAM (blue curves).

excitations in red in Figures 2a and 2b. Ocean current effects also agree well with residual *X* and *Y* variations over a broad band of frequencies and appear to be as important as OBP in driving polar motion. Figures 3a and 3b show combined oceanic effects ECCO OBP plus *U* and *V* (green) and T/P OBP plus ECCO *U* and *V* (red) compared with the residual *X* and *Y* (blue). Total ocean contributions, either ECCO OBP plus *U* and *V* or T/P OBP plus ECCO *U* and *V*, agree better with residual *X* and *Y* than either contribution separately.

[17] Annual and semiannual amplitudes and phases of the combined series are obtained by least squares, with results shown in Table 1. ECCO seasonal ocean current effects on *X* are greater than OBP and are similar in the *Y* component.

Table 2. Cross-Correlation Coefficients Between Intraseasonal Polar Motion (*X*, *Y*) Not Accounted for by the Atmosphere (SPACE2001-AAM) and Effects From the Oceans and Variance Reduction When Oceanic Excitations Are Removed From SPACE2001-AAM

	Polar Motion *X*: SPACE2001-AAM		Polar Motion *Y*: SPACE2001-AAM	
Excitation Source	Maximum Correlation	Reduced Variance, %	Maximum Correlation	Reduced Variance, %
ECCO OBP	0.65	40	0.72	46
T/P OBP	0.56	31	0.76	49
ECCO *U* and *V*	0.52	25	0.72	29
ECCO OBP plus *U* and *V*	0.76	57	0.79	60
T/P OBP plus ECCO *U* and *V*	0.68	46	0.81	63
OAM [*Gross et al.*, 2003]	0.73	52	0.63	40

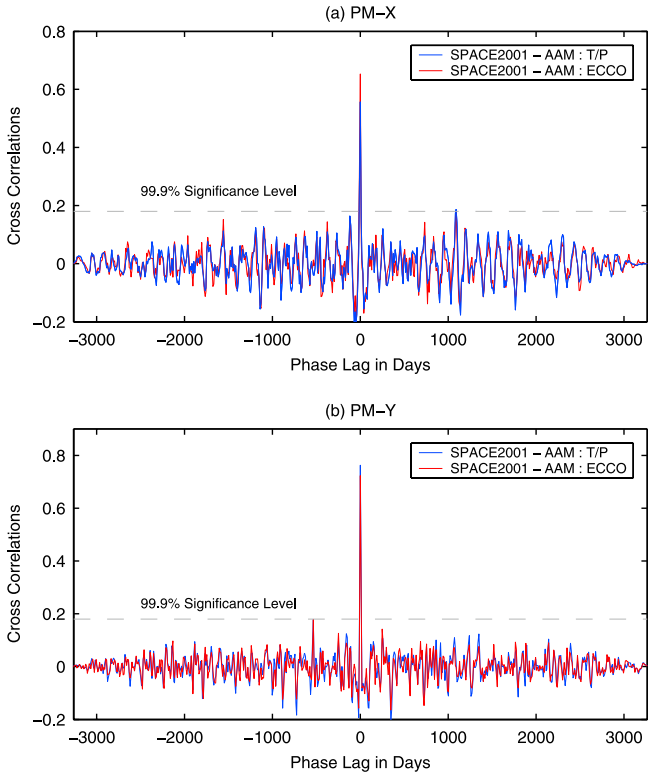

Figure 5. For (a) X and (b) Y cross correlation coefficients between T/P-derived OBP effects and residual X and Y (blue curves) and between ECCO OBP effects and residual X and Y (red curves).

Discrepancies at seasonal frequencies in Table 1 are expected because continental water storage change, not considered here, is likely to have an important effect on seasonal polar motion [e.g., *Chao and O'Connor*, 1988; *Kuehne and Wilson*, 1991; *Chen et al.*, 2000a]. Thus Table 1 mainly illustrates the relative size of individual and combined oceanic effects (OBP, current, and OBP plus current) on X and Y. To close the budget, effects from all sources (atmosphere, ocean, and continental water) need to be estimated in a fully consistent way.

[18] Figures 4a and 4b compare intraseasonal X and Y residuals and two combined oceanic excitations (i.e., ECCO OBP plus U and V and T/P OBP plus ECCO U and V). Combined OBP and ocean current effects improve the agreement with X and Y residuals. Thus oceanic mass redistribution and currents are major contributors to these nonatmospheric X and Y residuals.

4.3. Cross Correlation and Variance Analysis

[19] We compute normalized cross correlations between intraseasonal time series in Figures 2a, 2b, 4a, and 4b, with Table 2 giving the zero-lag correlation coefficients. Percentage variance reductions associated with subtracting each oceanic contribution from observed X and Y residuals are also listed in Table 2. As an example, Figures 5a and 5b show the cross correlation between (X, Y) and estimates from ECCO OBP and T/P OBP. Figures 5a and 5b and Table 2 show clearly that estimated OBP and current excitations are strongly correlated with nonatmospheric residual X and Y excitations. ECCO (OBP plus current) excitations show stronger correlations in X (0.76 versus 0.68) and explain a relatively larger portion of the variance (57% versus 46%). However, for Y, T/P OBP (plus ECCO currents) provides better agreement (0.81 versus 0.79) and explains more of the variance than the full ECCO estimate (63% versus 60%). Combined excitations, both ECCO OBP plus U and V and T/P OBP plus ECCO U and V can explain more variance than either OBP or currents separately.

[20] We also list in Table 1 very recent estimates of annual and semiannual amplitude and phase from the oceanic angular momentum time series published by *Gross et al.* [2003]. These are from an ECCO OGCM run that was not data-assimilating. These results are averaged and resampled at the same 10-day intervals and determined from exactly the same time period of 1993–2001. Cross correlation and variance reduction at intraseasonal timescales are also listed in Table 2 for these series. This non-data-assimilating ECCO run predicts relatively smaller annual excitation in X and slightly larger in Y compared with the data- assimilating ECCO calculation used in our study. Semiannual excitations estimated from the data-assimilating ECCO model (used in this study) and T/P

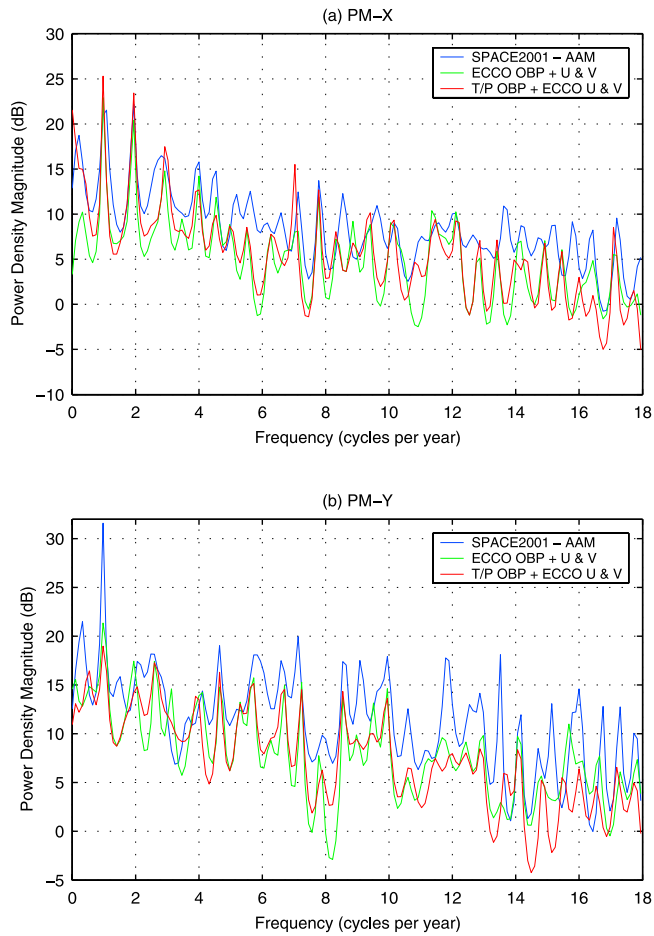

Figure 6. For (a) X and (b) Y power spectrum densities of residual (blue curves), contributions from ECCO OBP plus U and V (green curves), and T/P OBP plus ECCO U and V (red curves), estimated using the Burg method (with order of 72).

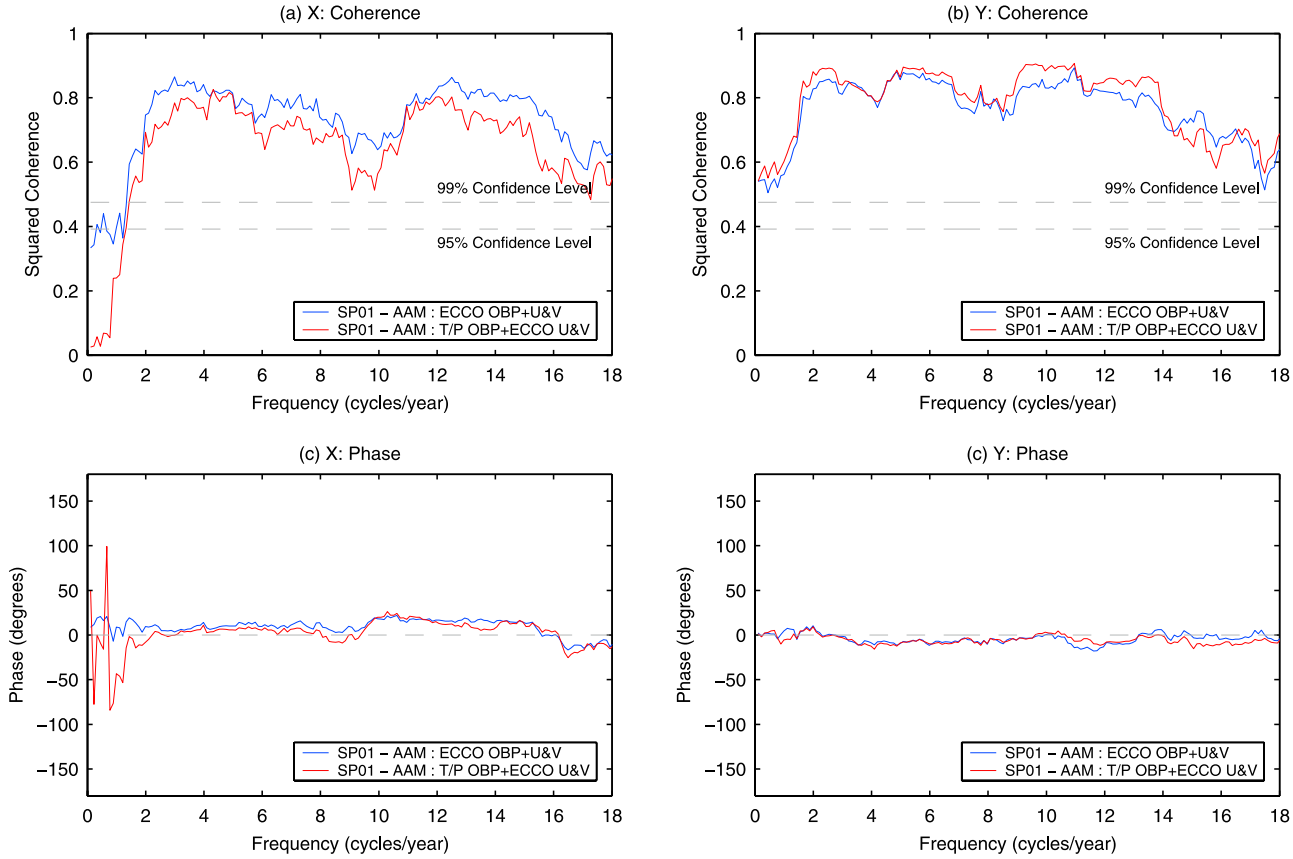

Figure 7. Magnitude for (a) *X* and (b) *Y* and phase of the squared coherence for (c) *X* and (d) *Y* of SPACE2001-NCEP AAM with oceanic excitations from ECCO OBP plus *U* and *V* (blue curves) and T/P OBP plus ECCO *U* and *V* (red curves). Annual and semiannual variations have been removed from all time series by least squares fitting. Mean and trend are also removed.

OBP (plus ECCO currents) agree apparently better with observations than those from the non-data-assimilating ECCO run. For the intraseasonal residuals, estimates from the data-assimilating ECCO and T/P OBP (plus ECCO currents) also agree significantly better (with observations) in terms of both correlation and variance reduction, especially in the *Y* component (see Table 2).

4.4. Power and Coherence Spectrum Analysis

[21] We compute power spectrum densities of nonatmospheric residuals in *X* and *Y* and compare them with spectra of the two combined estimates of oceanic contributions, shown in Figures 6a and 6b. At seasonal or shorter timescales, oceanic contributions agree well with SPACE2001-AAM residuals in *X* and *Y*. The annual variation appears dominant in both *X* and *Y*, while the semiannual variation is also significant in *X*. This is consistent with the values in Table 1.

[22] Figures 7a through 7d show magnitudes and phases of the coherence between nonatmospheric residuals and two oceanic excitations, ECCO OBP plus *U* and *V*, and T/P OBP plus ECCO *U* and *V*. Mean and trend are removed from all time series. Annual and semiannual variations have also been removed by least squares fitting. The two dashed lines in Figures 7a and 7b represent the 95% and 99% confidence levels. Both ECCO- and T/P-based excitations show good correlation with SPACE2001-AAM residuals over much of the intraseasonal frequency band. The ECCO estimates show better coherence with the SPACE2001-AAM residuals in *X*, while T/P (plus ECCO *U* and *V*) appears showing better agreement in *Y*. This is consistent with the results from cross correlation and variance reduction analysis (see Table 2).

5. Discussion

[23] Predictions from the data-assimilating ECCO model and T/P altimeter measurements show the oceans to be a major contributor to observed polar motion, especially at seasonal and intraseasonal timescales. Oceanic mass (OBP) and current changes are all important in affecting polar motion. The combined oceanic effects (on the basis of either ECCO or T/P plus ECCO) appear to be a major contributor to the remaining intraseasonal variations in *X* and *Y*. At annual period, ECCO and T/P plus ECCO can more than explain nonatmospheric *X* residuals and provide comparable estimates for *Y*. At the semiannual period the two estimates explain a majority of the residual signals, especially in *X* (see Figure 8 and Table 1).

[24] Compared with previous studies, we find improved agreement between estimates of ocean contributions and observed polar motion. The data-assimilating ECCO model estimates thus appear superior to the Parallel Ocean Climate Model (POCM) in modeling large-scale oceanic mass and

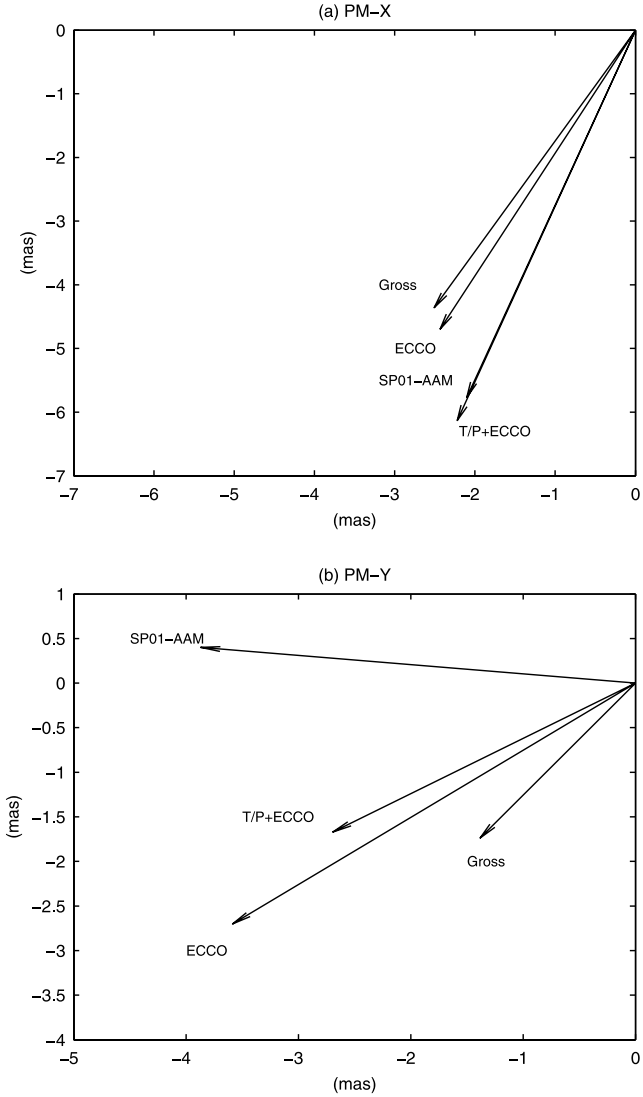

Figure 8. Phasor plots for semiannual variations estimated from SPACE2001-AAM residuals and oceanic excitations in (a) *X* and (b) *Y*.

current changes. The improvement in correlation coefficients is significant (e.g., 0.76/0.79 from this study versus 0.38 from that of *Johnson et al.* [1999], based on the POCM model). Our findings are in general agreement with those of *Gross et al.* [2003], based on the ECCO non-data-assimilating model. However, we find that the data-assimilating ECCO model used here leads to better agreement with observed polar motion (see Table 1). This is also true for the nonseasonal residuals (see Table 2).

[25] The T/P-based predictions (T/P OBP plus ECCO *U* and *V*) show significant improvement in agreement with *X* and *Y* residuals when compared with previous results [e.g., *Chen et al.*, 2000a]. This is attributed to the availability of a longer T/P data set and the employment of ECCO to estimate steric SSH. Steric effects account for a majority of observed sea level change [e.g., *Chen et al.*, 2000b] and are a critical element in using altimeter data to infer oceanic mass redistribution. The apparent success in estimating steric effects from ECCO demonstrates that altimeter observations can be a valuable data resource in studies of oceanic mass variations and redistribution.

[26] Agreement between OGCM predictions and observed polar motion is remarkably good, considering the possibilities for inadequacies in OGCM results. OBP current estimates, especially at depth, are virtually unconstrained by observations, so it is difficult to assess errors. The same goes for T and S, especially at depth. In the case of OBP, the difference between two temporally correlated quantities (SSH and SSH_{steric}) of about the same size, there is a good chance that errors will contaminate the estimates. The Bossiness approximation (conserving ocean volume) forces an ad hoc adjustment (the Greatbatch convention) to conserve mass. Nonglobal coverage of both the OGCM and T/P may be a problem as well. A mass-conserving OGCM [e.g., *Huang et al.*, 2001] that assimilates altimeter sea level, sea surface temperature, and salinity data and is driven by winds, fluxes, and atmospheric pressure is clearly the next step. In the longer term, fully coupled models that conserve mass within the full atmosphere-ocean-hydrosphere system are needed. Assimilation of satellite gravity observations, such as those from the Gravity Recovery and Climate Experiment mission, would likely be an important improvement in OGCM development as well.

[27] **Acknowledgments.** We thank Richard Gross, Thomas Johnson, and another anonymous reviewer for their insightful comments, which led to improvements in the presentation. We are grateful to the ECCO team for providing the model data, with special thanks to Zhangfan Xing and Benyang Tang for help in extracting and interpreting the data. We would like to thank Atmospheric and Environmental Research and their activities organized under the International Earth Rotation Service for providing the NCEP reanalysis AAM data. This research was supported by NASA's Solid Earth and Natural Hazards Program.

References

Barnes, R., R. Hide, A. White, and C. Wilson (1983), Atmospheric angular momentum functions, length of day changes and polar motion, *Proc. R. Soc. London, Ser. A*, *387*, 31–73.

Chao, B. F., and A. Y. Au (1991), Atmospheric excitation of the Earth's annual wobble: 1980–1988, *J. Geophys. Res.*, *96*, 6577–6582.

Chao, B. F., and W. P. O'Connor (1988), Effect of a uniform sea-level change on the Earth's rotation and gravitational field, *Geophys. J. R. Astron. Soc.*, *93*, 191–193.

Chen, J. L., C. R. Wilson, D. P. Chambers, R. S. Nerem, and B. D. Tapley (1998), Seasonal global water mass budget and mean sea level variations, *Geophys. Res. Lett.*, *25*(19), 3555–3558.

Chen, J. L., C. R. Wilson, B. F. Chao, C. K. Shum, and B. D. Tapley (2000a), Hydrologic and oceanic excitations to polar motion and length of day variation, *Geophys. J. Int.*, *141*, 149–156.

Chen, J. L., C. K. Shum, C. R. Wilson, D. P. Chambers, and B. D. Tapley (2000b), Seasonal sea level change from TOPEX/Poseidon observation and thermal contribution, *J. Geod.*, *3*, 638–647.

Chen, J. L., C. R. Wilson, X. G. Hu, and B. D. Tapley (2003), Large-scale mass redistribution in the oceans, 1993–2001, *Geophys. Res. Lett.*, *30*(20), 2024, doi:10.1029/2003GL018048.

Dickey, J. O., S. L. Marcus, C. M. Johns, R. Hide, and S. R. Thompson (1993), The oceanic contribution to the Earth's seasonal angular momentum budget, *Geophys. Res. Lett.*, *20*(24), 2953–2956.

Dickey, J. O., S. L. Marcus, O. de Viron, and I. Fukumori (2002), Recent Earth oblateness variations: Unraveling climate and postglacial rebound effects, *Science*, *298*, 1975–1977.

Eubanks, T. M. (1988), Combined Earth rotation series smoothed by a Kalman filter, in *Bureau International de l'Heure Annual Report for 1987*, pp. D85–D86, Obs. de Paris, Paris.

Eubanks, T. M. (1993), Variations in the orientation of the Earth, in *Contributions of Space Geodesy to Geodynamics—Earth Dynamics*, *Geodyn. Ser.*, vol. 24, edited by D. E. Smith and D. L. Turcotte, pp. 1–54, AGU, Washington, D. C.

Eubanks, T. M., J. A. Steppe, J. O. Dickey, R. D. Rosen, and D. A. Salstein (1988), Causes of rapid motions of the Earth's pole, *Nature*, *334*, 115–119.

Fofonoff, P., and R. C. Millard Jr. (1983), Algorithms for computation of fundamental properties of seawater, *UNESCO Tech. Pap. Mar. Sci.*, *44*, 53 pp.

Fukumori, I., T. Lee, D. Menemenlis, L.-L. Fu, B. Cheng, B. Tang, Z. Xing, and R. Giering (2000), A dual assimilation system for satellite altimetry, paper presented at Joint TOPEX/Poseidon and Jason-1 Science Working Team Meeting, NASA, Miami Beach, Fla., 15–17 Nov.

Greatbatch, R. J. (1994), A note on the representation of steric sea level in models that conserve volume rather than mass, *J. Geophys. Res.*, *99*, 12,767–12,771.

Gross, R. (2002), Combinations of Earth orientation measurements, SPACE2001, COMB2001, and POLE2001, *JPL Publ., 02-08*, 27 pp.

Gross, R. S., I. Fukumori, and D. Menemenlis (2003), Atmospheric and oceanic excitation of the Earth's wobbles during 1980–2000, *J. Geophys. Res.*, *108*(B8), 2370, doi:10.1029/2002JB002143.

Hide, R., and J. O. Dickey (1991), Earth's variable rotation, *Science*, *253*, 629–637.

Huang, R. X., X.-Z. Jin, and X.-H. Zhang (2001), An ocean general circulation model in pressure coordinates, *Adv. Atmos. Sci.*, *18*, 1–22.

Jet Propulsion Laboratory (2002), *Sea Surface Temperature and Height, Global 0.5 and 1.0 Deg Grids* (*JPL, WOCE v3*) [DVD-ROM], Pasadena, Calif. (Available at http://podac.jpl.nasa.gov/woce)

Johnson, T. J., C. R. Wilson, and B. F. Chao (1999), Oceanic angular momentum variability estimated from the Parallel Ocean Climate Model, 1988–1998, *J. Geophys. Res.*, *104*, 25,183–25,195.

Kalnay, E., et al. (1996), The NCEP/NCAR 40-year reanalysis project, *Bull. Am. Meteorol. Soc.*, *77*, 437–471.

Kuehne, J., and C. R. Wilson (1991), Terrestrial water storage and polar motion, *J. Geophys. Res.*, *96*, 4337–4345.

Minster, J. F., A. Cazenave, Y. V. Serafini, F. Mercier, M. C. Gennero, and P. Rogel (1999), Annual cycle in mean sea level from TOPEX-Poseidon and ERS-1: Inference on the global hydrological cycle, *Global Planet. Change*, *20*, 57–66.

Ponte, R. M., and A. H. Ali (2002), Rapid ocean signals in polar motion and length of day, *Geophys. Res. Lett.*, *29*(15), 1711, doi:10.1029/2002GL015312.

Ponte, R. M., and D. Stammer (1999), Role of ocean currents and bottom pressure variability on seasonal polar motion, *J. Geophys. Res.*, *104*, 23,393–23,410.

Ponte, R. M., D. Stammer, and J. Marshall (1998), Oceanic signals in observed motions of the Earth's pole of rotation, *Nature*, *391*, 476–479.

Ponte, R. M., D. Stammer, and C. Wunsch (2001), Improving ocean angular momentum estimates using a model constrained by data, *Geophys. Res. Lett.*, *28*(9), 1775–1778.

Salstein, D. A., and R. D. Rosen (1997), Global momentum and energy signals from reanalysis systems, paper presented at 7th Conference on Climate Variations, Am. Meteorol. Soc., Boston, Mass.

Wilson, C. R. (1985), Discrete polar motion equations, *Geophys. J. R. Astron. Soc.*, *80*, 551–554.

J.-L. Chen, B. D. Tapley, and C. R. Wilson, Center for Space Research, University of Texas at Austin, 3925 W. Braker Lane, Suite 200, Austin, TX 78759-5321, USA. (chen@csr.utexas.edu; tapley@csr.utexas.edu; crwilson@mail.utexas.edu)

X.-G. Hu and Y.-H. Zhou, Shanghai Astronomical Observatory, Chinese Academy of Sciences, Shanghai 200030, China. (hxg@center.shao.ac.cn; yhzhou@center.shaso.ac.cn)